Published in final edited form as:
J Thromb Haemost. 2010 May ; 8(5): 1066–1074. doi:10.1111/j.1538-7836.2010.03802.x.

The spatial dynamics of fibrin clot dissolution catalyzed by erythrocyte-bound vs. free fibrinolytics

K. C. GERSH[*], **S. ZAITSEV**[†,‡], **V. MUZYKANTOV**[†,‡], **D. B. CINES**[§], and **J. W. WEISEL**[*]

[*]Department of Cell & Developmental Biology, University of Pennsylvania School of Medicine, Philadelphia, PA, USA

[†]Institute for Environmental Medicine, University of Pennsylvania School of Medicine, Philadelphia, PA, USA

[‡]Department of Pharmacology, University of Pennsylvania School of Medicine, Philadelphia, PA, USA

[§]Department of Pathology and Laboratory Medicine, University of Pennsylvania School of Medicine, Philadelphia, PA, USA

Summary

Background—Coupling fibrinolytic plasminogen activators to red blood cells (RBCs) has been proposed as an effective, yet safe method of thromboprophylaxis, because of increased circulation lifetime and reduced propensity to induce hemorrhage by selectivity for nascent thrombi rather than pre-formed hemostatic clots.

Objectives and methods—We used confocal microscopy of fluorescently labeled fibrin and erythrocytes in plasma-derived clots to study the spatial dynamics of lysis catalyzed by RBC-coupled vs. free plasminogen activators (RBC-PA vs. PA).

Results—Clot lysis catalyzed by free PA progressed gradually and uniformly. In contrast, distinct holes formed surrounding RBC-PA while the rest of the clot remained intact until these holes enlarged sufficiently to merge, causing sudden clot dissolution. Compared with naïve RBCs within clots lysed by free PA, RBC-PA moved faster inside the fibrin network prior to clot dissolution, providing a potential mechanism for spatial propagation of RBC-PA induced lysis. We also showed the focal nature of fibrinolysis by RBC-PA as dense loading of PA onto RBCs initiates more efficient lysis than equal amounts of PA spread sparsely over more RBCs. In an *in vitro* model of clots exposed to buffer flow, incorporated RBC-PA increased permeability and formed channels eventually triggering clot dissolution, whereas clots containing free PA remained intact.

Conclusions—Clot lysis by RBC-PA begins focally, has a longer lag phase when measured by residual mass than homogeneous lysis by PA, is propagated by RBC-PA motility and provides more effective clot reperfusion than free PA, making RBC-PA attractive for short-term thromboprophylaxis.

Keywords

erythrocytes; fibrin; fibrinolysis; plasminogen activators

Correspondence: John W. Weisel, Department of Cell & Developmental Biology, University of Pennsylvania School of Medicine, 1054 BRB II/III, 421 Curie Blvd, Philadelphia, PA 19104-6058, USA. Tel.: +1 215 898 3573; fax: +1 215 898 9871. weisel@mail.med.upenn.edu.

Introduction

Post-surgical patients present a high risk for both thrombosis and bleeding [1]. For this reason, thromboprophylaxis often falls short in post-operative and other high-risk settings, for example massive trauma and stroke [2]. These and other patients would benefit from a method of short-term thromboprophylaxis that averted the formation of occlusive thrombi, while ensuring survival of pre-formed hemostatic clots and preventing intracranial hemorrhage. Plasminogen activators (PAs), potent anti-thrombotic agents that promote fibrinolysis, are generally not administered prophylactically because of a high incidence of intracranial bleeding [1] and extremely short half-life [3]. Coupling of tissue plasminogen activator (tPA) or urokinase-type PA (uPA) to a red blood cell (RBC-tPA or RBC-uPA) provides a 'Trojan horse-like' strategy for drug delivery by incorporating within nascent clots while preventing penetration of pre-existing clots *in vivo* [4,5]. In animal models of arterial and venous thrombosis, systemic prophylactic administration of RBC-tPA prevented formation of occlusive thrombi, without dissolving hemostatic mural clots [4,6]. Additional *in vivo* studies have shown that RBC-tPA provides cerebrovascular thromboprophylaxis, prevents tPA extravasation into the central nervous system and substantially reduces the hemorrhagic risk associated with free tPA [7]. Extensive work has been performed to characterize and improve the pharmacokinetic profile of RBC-PA, including conjugation of PAs to antibody fragments that bind the drug directly to circulating RBCs after intravenous injection [6,8,9].

These studies affirmed the potential of RBC-PA as an effective and safe intervention for short-term thromboprophylaxis. However, we still know very little about the spatial dynamics of clot dissolution by RBC-PA, in particular, how RBC-PA interacts with fibrin fibers and catalyzes fibrinolysis.

Fibrinolysis takes place when the active enzyme plasmin cleaves fibrin fibers. Plasmin is generated from proteolytic cleavage of plasminogen by a PA. Cleavage of fibrin produces free C-terminal lysines that serve as binding sites for plasminogen and PA and create a positive feedback loop to enhance plasmin generation. Hemostatic balance is maintained by suppression of fibrinolysis by inhibitors [10,11].

Our laboratory has used confocal microscopy to analyze clot structure during fibrinolysis in real time [12]. When tPA was introduced extrinsically to the edge of a pre-formed clot, imitating the clinical mode of action, the lysis rate was influenced by binding, enzymatic reactions and movement of the enzyme into the clot as a function of network architecture, with faster movement for coarse rather than fine fiber networks [12]. During intrinsic lysis, a physiological model in which tPA and plasminogen were incorporated during clot formation, fibrinolysis occurred throughout the clot. Although this mode of tPA administration is not attainable post-thrombosis, from a mechanistic viewpoint it was important that the events involved were similar to those seen at the lysis front during external lysis [13].

In the current investigation, our goal was to determine the detailed spatial dynamics of fibrinolysis catalyzed by RBC-PA compared with free PA. We used laser scanning and spinning disk confocal microscopy to obtain dynamic images of naturally hydrated clots during fibrinolysis. We determined that both RBC-PA and free PA destroy fibrin fibers, but overall network dissolution was fundamentally different. Lysis is localized around RBC-PAs until individual holes merge resulting in precipitous dissolution, and RBCs coated with PA at high density are more effective than their low density counterparts at the same total dose. Furthermore, RBC-PA, but not free PA, restored perfusion through clots exposed to flow, a finding of high potential clinical relevance.

Materials and methods

Preparation of human PPP and RBCs

Human platelet-poor plasma (PPP) and human RBCs (hRBCs) were prepared as described [14]. Percent RBCs was determined by volume after centrifugation. RBCs were fluorescently labeled according to the manufacturer's protocol with Vybrant DiD (A_{max} = 644 nm) or Vybrant DiO (A_{max} = 484 nm) cell-labeling solution (Molecular Probes, Eugene, OR, USA).

Preparation of mouse RBCs

Mouse blood was collected as described [9]. Mouse RBCs (mRBCs) were prepared from whole blood, stored and labeled as described for hRBCs, except that they were washed three times.

Preparation of RBC-PA and free PA

To bind PA to RBCs, we used a recombinant low-molecular weight single chain uPA (L144-L411) fused with the single chain variable fragment (scFv) of an antibody to mRBC (scFv-uPA). The plasmin-sensitive cleavage site (F157, K158) has been replaced with a thrombin-sensitive cleavage site (P155, R156) by deleting residues Phe157 and Lys158 as described for a similar fusion [15]. The scFv of rat monoclonal antibody Ter119 that recognizes murine glycophorin A, expressed on the surface of mRBCs [16] has been fused with thrombin-activatable low-molecular weight single chain uPA using a linker peptide ($(SSSSG)_2AAA$), as we have recently described [17] (Fig. 1). To load approximately 40 000 molecules of PA per RBC, 0.360 μM of the PA fusion was mixed with 10% mRBCs for 1 h at room temperature, rotating at 8 rpm. Changing the amount of added PA varied loading density. During loading, PA was activated with 0.1 U mL^{-1} human α-thrombin. Afterwards, cells were spun down and washed three times with phosphate-buffered saline (PBS; Dulbecco's, Invitrogen, Carlsbad, CA, USA) to remove thrombin and excess conjugate, then resuspended to a 10% hematocrit in PBS. For samples of free PA mixed with RBCs, the PA construct was activated with thrombin, then mixed with hRBCs, which are not recognized by the scFv.

Amidolytic assay

RBC-PA activity was measured with a chromogenic amidolytic activity assay. We prepared a calibration curve of 0.0205 μM – 0.164 μM free PA with 1% mRBCs in PBS to convert results from absorbance units to activity. Samples containing 1% RBC-PA were also prepared in PBS. To a 100-μL sample or standard, we added 50 μL of 2.5 mM Spectrozyme UK (American Diagnostica, Stamford, CT, USA) and rotated the tubes for 25 min. The RBCs were spun down and the supernatant transferred to cuvettes. The reactions were quenched with 50 μL of 50% acetic acid and absorbance was read at 405 nm using a Beckman Coulter DU640 spectrophotometer.

Spinning disk confocal microscopy

Clots were prepared using PPP mixed with 0.075 mM (final conc.) Alexa 488-labeled human fibrinogen (Molecular Probes, molar ratio of dye/protein = 8:1). Clot formation was initiated by addition of thrombin and $CaCl_2$ to final concentrations of 0.5 U mL^{-1} and 20 mM, respectively. We prepared thin chambers (~200 μM) composed of a coverslip supported on a microscope slide by double-sided tape. DiO-labeled RBC-PA (1%) or DiO-labeled hRBCs (1%) + free PA (0.00820 μM) (all final concs) were mixed into the sample, thrombin was added, and image acquisition began within 3–6 min. Images were acquired on a spinning disk confocal microscope with a Yokogawa CSU10 scanner combined with an Olympus (Center Valley, PA, USA) IX71 microscope using a 60× water (1.20 NA) objective. We took 5 μM confocal stacks every 10 s.

Laser scanning confocal microscopy

Clots and chambers were prepared as for spinning disk confocal microscopy, except that RBCs were labeled with DiD so they could be visualized in a separate channel from Alexa 488-labeled fibrin. Microscopy was performed as described [14].

Image analysis

Images were opened and manipulated in Image J (Wayne Rasband, NIH) and presented as Z-projections with the RBC channel overlaying the fiber channel. Network structures were quantified using the fiber channel only with the image processing program Metamorph's (Molecular Devices, Down-ingtown, PA, USA) Adaptive Background Correction System. We entered parameters for minimum and maximum fiber width and brightness difference between fibers and background, then adjusted these values until the program generated a mask that closely overlaid the fibrin network. This mask determined the fibrin in each image to measure % lysis over time (Fig. S1A). Movement of RBCs was measured using the RBC channel only. To randomly select RBCs to track, we overlaid a grid over the first time point and highlighted any RBCs that intersected its lines. We then measured the X-Y coordinate of the center of the cell and the Z slice where it was the brightest over each time point to provide a three-dimensional description of the cell's movement {distance = $\sqrt{[(x_2-x_1)^2 + (y_2-y_1)^2 + (z_2-z_1)^2]}$} (Fig. S1B).

Clot permeability

Permeation experiments were performed as described [15], with the following modifications: clots were prepared with 2% DiD-labeled RBC-PA or 2% DiD-labeled hRBCs + free PA mixed into PPP, and clot formation was triggered by addition of 1U mL^{-1} thrombin. After 10 min, clots were removed from the rotator, topped with permeation buffer and attached to tubing extending from a reservoir set above the clot. Permeation buffer was PBS with 0.25% DiO-labeled hRBCs. Flow through the clot was collected into tared tubes starting immediately and tubes were exchanged every 1–4 min until the clot ruptured. Permeability constants were determined as described [14]. Samples (100 μL) of the column flow-through were placed in MatTek (Ashland, MA, USA) dishes containing a no. 1.5 coverslip. Images of the eluted cells were obtained using excitation at both 488 nm and 647 nm.

Results

Spatiotemporal differences in fibrinolysis mediated by free PA vs. RBC-PA

The therapeutic target for RBC-PA is a nascent thrombus into which it incorporates during clotting [4]. We simulated this situation by mixing pooled PPP with RBC-PA or free PA, prior to adding thrombin to initiate clot formation. While free PA injected *in vivo* prior to clotting will not incorporate into new clots as effectively as long-circulating RBC-PA, our *in vitro* model allowed us to compare dissolution of clots by similarly effective doses of RBC-bound and free PA.

We used spinning disk confocal microscopy to monitor lysis of a naturally hydrated fibrin clot. We kept the total %RBCs constant to achieve a similar clot structure [14]; hence naïve human RBC were added along with the PA fusion protein in the samples lysed by free PA. Figure 2 shows lysis catalyzed by free PA (i) or RBC-PA (ii). Complete movies of these two lysis reactions are included in Supporting information (Fig. S2).

These images demonstrate significant differences in lysis. First, hRBCs (Fig. 2A) are larger than mRBCs (Fig. 2B) (mean corpuscular volume, hRBCs ~88 μM^3; mRBCs ~50 μM^3) [18]. Second, at the PA concentrations used, clot dissolution occurred faster with free PA than with RBC-PA (25 vs. 41 min in the experiment shown), probably because of the higher diffusability

of free enzyme. However, there were major morphological differences between these two reactions with respect to how the fibrin networks disassembled. With free PA, fibrin fibers broke homogeneously throughout the clot, and as time progressed, the clot melted away, essentially uniformly and gradually. In contrast, fiber dissolution by RBC-PA was spatially restricted to the sites around the RBC-PAs themselves, whereas areas distant from RBC-PA remained intact throughout the early and intermediate time points. This spatial restriction of fibrinolysis led to the formation of holes surrounding the RBC-PA. Once these holes enlarged sufficiently to merge, the RBC-PA trapped in each hole were freed to sweep over the remaining parts of the clot leading to rapid dissolution, after the prolonged lag at the reaction's inception.

To quantify fibrin network dissolution, we monitored fibrinolysis with the laser scanning confocal microscope. Although we could only acquire images every minute, we imaged fibers and RBCs in separate channels. The amount of free PA (0.00902 μM, final conc) included in this representative reaction (Fig. 3A) was adjusted so complete network dissolution would occur close to when it was observed for RBC-PA (Fig. 3B) [movies in Supporting information (Fig. S3)]. This imaging technique confirmed the differences in lysis progression between free and RBC-bound PA that we observed with spinning disk microscopy, Fig 2. Note that the number of RBC-PAs visible at 26 min increased drastically because RBCs settled as the network above the field of view collapsed.

We measured the percentage of clot lysed over time, and the first time point when no fibrin fibers were visible was designated as 100% lysis (preliminary time points corresponding to clot formation are not shown). In order to compare data from multiple experiments in which different total amounts of PA had been added, we converted time in minutes to % time required for complete network lysis using this determination of 100% lysis for six RBC-PA and ten free PA-catalyzed reactions (Fig. 3C). The two averaged lysis curves differed significantly in the intermediate time points, reflecting the qualitative differences observed in the confocal images. This plot shows that while both reactions displayed a steep increase in lysis rate during the last few time points, the RBC-PA clot remained relatively intact during intermediate time points while the rate of lysis induced by free PA increased more steadily.

RBC movement

Upon observing that RBC-PA serve as apparent lysis foci, we wondered whether RBC-PA are stably mounted within the fibrin matrix, or free to move. To address this question, we measured RBC movement by determining the X, Y, and Z coordinates of individual RBCs over time and converting the data to a minimum velocity by calculating the distance moved between time points (Supplemental Fig. S4).

Figure 4 shows RBC movements plotted vs. the relative scale of % time required to achieve complete lysis. Velocity of hRBCs in intact clots not undergoing lysis was close to zero throughout the duration of observation (data not shown). At early and intermediate time points, the naïve hRBCs incorporated into a clot along with free PA displayed similarly low velocity. Then after approximately 70% of the time to lysis, the hRBC velocity increased drastically. This spike in RBC movement corresponded to the precipitous destruction of the fibrin network (Fig. 3C) that released passively entrapped RBCs.

RBC-PA movement was very different. During early and intermediate time points, RBC-PA moved within the clots significantly faster than the bystander hRBCs in clots lysed by free PA. At later time points, RBC-PA motility had not yet spiked like the bystander hRBCs in clots that had undergone more extensive lysis by free PA. Therefore, while they eventually attained the same apparent final velocity (~19 $\mu M\ min^{-1}$), RBC-PA did so much more gradually than bystander hRBCs.

To determine if movement was solely as a result of RBC settling by gravity, we plotted the Z-directional movement over time for each RBC in each image (data not shown). Both upward and downward movements were observed without an overriding trend. Thus during clot dissolution, RBCs are acted upon by both gravity and other forces. Mouse RBCs are smaller than human RBCs (5 μM vs. 7 μM) and, therefore, might have a higher diffusion constant. We tested whether the higher velocity of mRBC-PA vs. hRBC plus free PA during early stages of lysis were as a result of this difference in diffusion rate rather than the effect of PA binding to the mRBC. We labeled mRBCs and hRBCs with different fluorophores, mixed them with samples of PPP and free tPA (which will not bind to either species' RBCs), formed clots by adding thrombin, and monitored hRBC and mRBC movement over time as the clot was lysed by the action of free tPA. hRBCs and mRBCs moved at the same rate at greater than 93% of the time points measured for three separate clots. Compared with the extensive differences in movement of free and bound uPA shown in Figure 4, we conclude that the difference in RBC size has little impact on RBC movement during fibrinolysis.

Density of PA loading onto RBCs affects lysis rate

To determine whether the density of PA loading onto an RBC affected fibrinolysis, we visualized fibrinolysis of clots prepared with equal total doses of PA, but spread over many sparsely loaded RBC-PAs, or over fewer more densely loaded RBC-PAs. To keep the total number of RBCs in each sample constant, we added labeled, unconjugated mRBCs to the high loading sample. Because loading density varies slightly among RBC-PA preparations, we did not average lysis curves; Figure 5 shows representative results from four experiments, each with different loading densities. In the experiment shown, the sparsely loaded RBC-PA sample had a specific activity of 2.4×10^{-11} μmol min^{-1} per RBC and the densely loaded sample had a specific activity approximately two times higher, as determined by an amidolytic assay performed just before use. Percent clot lysis was plotted against time in minutes for each clot studied. With the same total dose of PA in the clot, the densely loaded RBC-PAs catalyzed lysis faster than the sparsely loaded RBC-PA.

Monitoring fibrinolysis by measuring permeation of cell-containing buffer

The purpose of fibrinolytic therapy is to restore blood flow, especially oxygen-carrying RBCs, to ischemic tissue. We used permeation of RBC-containing buffer through a clot to model vessel reperfusion after thrombotic occlusion. We simulated clinical drug administration by forming a clot containing either free PA or RBC-PA and starting buffer flow soon after clot formation. We measured porosity of the sample by the permeation constant. Without any PA, buffer flow through a clot began slowly and became virtually non-existent (from $K_s \approx 4 \times 10^{-9}$ to 2×10^{-10} cm^2) as the RBCs in the permeation buffer formed a plug atop the clot. In contrast, when RBC-PA was incorporated into the clot, permeability instead increased over time until the clot lysed and fell out of the plastic tubing. As shown in Fig 6A,B, the RBC-PA permeability curve shape closely mirrors the lysis curve obtained by confocal microscopy for static clots using this same amount of RBC-PA.

Permeability experiments with free PA gave strikingly different results. At high concentrations of free PA, a stable clot did not form, so permeation could not be measured. However, once the amount of free PA was reduced such that the clot did not lyse before attachment to the buffer reservoir, permeability decreased over time until it was only slightly higher than that of a control non-lysing clot ($K_s \leq 2 \times 10^{-8}$ cm^2), and during 1 h of monitoring the clot never dissolved. This lack of reperfusion contrasts sharply from the dissolution of fibrin observed by microscopy triggered by addition of the same total amount of free PA without flow (Fig. 6A,B) and may reflect removal of free PA from the clot network.

While permeability of a lysing clot to liquid reflects density of the fibrin network, *in vivo* we are especially concerned with reperfusion of blood cells through an occlusive thrombus. To measure this property in the permeability system, we labeled the hRBCs initially incorporated into the clot with a different fluorescent label from those in the perfusion buffer. This allowed us to discern RBCs that permeated the entire clot from those that only washed out from the clot interior. In the non-lysing control sample, no buffer-derived RBCs moved through the clot at all during the monitored 35-min permeation (Fig. 6C). With free PA incorporated, occasional RBCs traveled from the perfusion buffer through the clot, but as buffer permeability leveled off, the number of RBCs passing through the clot decreased. In contrast, large numbers of buffer-derived RBCs traversed clots lysed by RBC-PA. This passage through the clot began almost immediately and well before the sample was dissolved enough to fall out of the permeability chamber.

Discussion

Our results indicate that both RBC-PA and free PA entrapped within a forming plasma clot cause fibrinolysis, but they destroy the clot via different pathways. *In vivo*, prophylactically administered RBC-PA is hypothesized to lyse nascent thrombi from within. This 'Trojan horse' model of thromboprophylaxis differs from conventional therapeutic thrombolysis of free PA injected post thrombosis. In the latter case, Collet *et al*. [12] noted that extrinsic lysis emanates as a front from the edge of a clot, and Sakharov and colleagues described a 'pre-lysis zone' where plasminogen bound to fibrin fibers beyond the lysis front before the clot dissolved [19]. In contrast, when the PA was incorporated inside a clot, lysis proceeded throughout the clot, rather than along an identified front [12]. During `pre-lysis,' plasminogen bound to nicked fibrin fibers causing minimal changes in clot structure. During 'final lysis,' the entire structure of the clot collapsed and dissolved [19]. Confocal microscopy revealed that during intrinsic lysis, fibers are laterally transected, they agglomerate to cause a transient increase in fiber diameter and then the fibrin network collapses into degradation products [13].

We have shown that lysis catalyzed by free PA in the presence of non-target hRBCs takes place according to the reported scenario of intrinsic lysis by free tPA [13,19], in which fibers are cleaved throughout the clot and the resulting fragments agglomerate and eventually dissolve. In contrast to this evenly distributed process, RBC-PA incorporated into the clot serve as foci of fibrinolytic activity and eventually lyse the entire clot throughout its bulk. Within the network, however, at early and intermediate time points, lysis progresses by the movement of small fronts extending out from each RBC-PA. We have no evidence to suggest whether fiber transection differs from the mechanisms previously observed with free tPA [12]. Lysis triggered by RBC-PA, therefore, occurs as a combination of intrinsic and extrinsic pathways.

We quantified these differences by measuring the fibrin network present at each time point during lysis (Fig 3C). These results clearly demonstrate the spatiotemporal differences between intermediate phases of lysis catalyzed by RBC-PA compared with free PA. While both RBC-PA and free PA display a pre-lysis phase and a fast final lysis stage when the clot disappears, there is a significant difference in the transition between these two phases. With free PA, the clot begins to dissolve relatively early, with the transition to final lysis taking place somewhere around 40% of the time it takes to complete lysis. The RBC-PA pre-lysis phase is much longer, and large-scale network changes do not start to occur until around 80% of the time to complete lysis. Immobilization of PA onto the RBC likely causes this delay in the onset of final lysis by restricting its diffusional accessibility to plasminogen. Although fibers located within close proximity of the trapped RBC-PA are lysed during this stage, an essential step in the eventual propagation of overall lysis, little change is visible on the fibrin network as a whole. Thus at intermediate time points, clots being lysed by free PA show more extensive lysis morphologically than those exposed to RBC-PA.

The rate of fibrinolysis is dependent upon the density of PA loading onto the RBC. Specifically, at all the loading densities we analyzed, from 1.5×10^{-11} to 4.8×10^{-11} μmol min^{-1} per RBC, the more densely loaded the RBC, the faster lysis occurs, even when the same total amount of PA is spread among a greater number of sparsely loaded RBCs (Fig. 5). We suggest that this rate difference is as a result of more effective activation of plasminogen, probably because of local overwhelming of the inhibitors (e.g. PAI-1) distributed throughout the clot by a high local concentration of PA on densely loaded RBC-PA. In fact, RBC-bound tPA is also partially preserved from inhibitors by the RBC glycocalyx [20].

We noticed conspicuous RBC-PA movement during fibrinolysis, especially at early stages of clot dissolution. Quantitative measurements showed that before significant portions of the network had degraded (up to ~55% time to lysis), RBC-PA were significantly more mobile than hRBCs with free PA (Fig 4). At this stage, the RBC-PA were moving as expected for free diffusion of a particle the size of an mRBC, whereas the hRBCs were trapped well below the rate of free diffusion for an hRBC. At later stages when the network containing free PA was more extensively dissolved than the one containing RBC-PA, the relative rates of movement reversed, and both types of cells sped up as the network dissolved.

An intriguing question about the mechanism of thromboprophylaxis by RBC-PA is how fibrinolysis by PA immobilized on a large carrier is efficiently propagated in spite of the obvious restrictions imposed by the fibrin meshwork on RBC-PA diffusability. Our somewhat surprising observation that RBC-PAs were more mobile than free RBCs prior to clot destruction (Fig 4) can be explained by our finding that the fibrin network is selectively lysed around the RBC-PAs (Fig 2B, 3B), whereas lytic events caused by free PA are spread more evenly throughout the clot. These results suggest that enhanced mobility of RBC-PA during the early phase of lysis prior to clot destruction is an important feature underlying the high efficacy of fibrinolysis by RBC-PA observed *in vivo* in animal models of thrombosis [4,7]. As fibers are cut by plasmin, tension is released [21] and the fibrin network rearranges [13,19]. These fiber movements batter the RBCs located in and around the fibrin network. In these regions of concerted lysis around RBC-PA, increased network movement propels the RBC-PA around the clot, and in so doing, propagates lysis.

While the microscopy performed in a static system gives us a clear picture of the spatiotemporal dynamics of lysis (and perhaps the reason why hemostatic clots are more resistant to RBC-PA than to free PA, especially after extensive cross-linking and retraction), permeation studies demonstrate that exposure to buffer flow differentially affects clots lysed by RBC-PA and free PA. The plot of permeation constant vs. time is akin to a plot of % lysis vs. time because both reflect breakdown of the fibrin network (Fig. 6A,B). We found that the shape of the permeation plot for RBC-PA is similar to that of the % lysis plot by microscopy, with final lysis in the permeability system occurring just before lysis in the microscopy system. A striking difference, however, exists for free PA, which effectively lysed the static microscopy clot, but did not increase permeability of the clot to flowing buffer. We propose that free PA is quickly washed away from the clot when it is exposed to flow. This is in stark contrast to RBC-PA, which remains trapped in the fibrin network even after flow begins, allowing it to trigger fibrin degradation providing perfusion of both liquid and RBCs prior to clot dissolution.

By separately labeling the RBCs that originated in permeation buffer from those that originated in the clot, we were able to discern the point at which a channel formed to allow fast permeation of RBCs through the clot. Inclusion of RBC-PA allows passage of buffer-derived RBCs early on, even before the clot has dissolved enough to be dislodged from the tube. With free PA, buffer-derived RBCs do begin to penetrate the clot, but their numbers never approach those seen with clots lysed by RBC-PA, and at later time points, transport drops off again as a plug of RBCs forms atop the clot. *In vivo* studies showed that RBCs carrying diverse PA derivatives,

but not their free PA counterparts (all of which have insufficiently short half-lives to be of utility in clinical thromboprophylaxis) effectively mediate vascular reperfusion [4,7,9]. The RBC-bound fibrinolytics used in these studies (tPA [4,6,7], retavase lacking fibrin affinity [6], uPA [5] and PA fusion proteins [17]) differ in their fibrin affinity, PAI-1 sensitivity and interaction with receptors. Nevertheless, the outcome was similar in all cases: RBC-bound, but not free PA provided prophylactic thrombolysis and reperfusion. Our present results support the notion that this effect is mediated by fibrinolysis from inside the clot, generating channels of sufficient size for blood perfusion. Certainly, the particular parameters of prophylactic thrombolysis attained by diverse versions of fibrinolytic drugs coupled to RBC may differ. However, our present results provide a mechanistic basis for the advantage of using RBC-PA for thromboprophylaxis and show the importance of taking flow and cell permeation into consideration when modeling clot lysis.

Supplementary Material

Refer to Web version on PubMed Central for supplementary material.

Acknowledgments

We thank Dr B. Ding and Ms S. Ismail for procurement of mRBCs and Dr R. Litvinov for assistance with editing of the manuscript.

Funding

RO1-HL090697 (V. Muzykantov); 5-T32-HL007971-06, HL076406, HL82545, HD57355, and a grant from the Penn Institute for Translational Medicine and Therapeutics (D. B. Cines); AHA-SDG-0535258N (SZ); HL030954 (J. W. Weisel).

References

1. Selim M. Perioperative stroke. N Engl J Med 2007;356:706–13. [PubMed: 17301301]
2. Clagett GP, Anderson FA Jr, Heit J, Levine MN, Wheeler HB. Prevention of venous thromboembolism. Chest 1995;108:312S–34S. [PubMed: 7555186]
3. Baruah DB, Dash RN, Chaudhari MR, Kadam SS. Plasminogen activators: a comparison. Vascul Pharmacol 2006;44:1–9. [PubMed: 16275118]
4. Murciano JC, Medinilla S, Eslin D, Atochina E, Cines DB, Muzykantov VR. Prophylactic fibrinolysis through selective dissolution of nascent clots by tPA-carrying erythrocytes. Nat Biotechnol 2003;21:891–6. [PubMed: 12845330]
5. Murciano JC, Higazi AA, Cines DB, Muzykantov VR. Soluble urokinase receptor conjugated to carrier red blood cells binds latent prourokinase and alters its functional profile. J Control Release. 2009 ????: ????–????
6. Ganguly K, Krasik T, Medinilla S, Bdeir K, Cines DB, Muzykantov VR, Murciano JC. Blood clearance and activity of erythrocyte-coupled fibrinolytics. J Pharmacol Exp Ther 2005;312:1106–13. [PubMed: 15525799]
7. Danielyan K, Ganguly K, Ding BS, Atochin D, Zaitsev S, Murciano JC, Huang PL, Kasner SE, Cines DB, Muzykantov VR. Cerebrovascular thromboprophylaxis in mice by erythrocyte-coupled tissue-type plasminogen activator. Circulation 2008;118:1442–9. [PubMed: 18794394]
8. Ganguly K, Goel MS, Krasik T, Bdeir K, Diamond SL, Cines DB, Muzykantov VR, Murciano JC. Fibrin affinity of erythrocyte-coupled tissue-type plasminogen activators endures hemodynamic forces and enhances fibrinolysis in vivo. J Pharmacol Exp Ther 2006;316:1130–6. [PubMed: 16284278]
9. Zaitsev S, Danielyan K, Murciano JC, Ganguly K, Krasik T, Taylor RP, Pincus S, Jones S, Cines DB, Muzykantov VR. Human complement receptor type 1-directed loading of tissue plasminogen activator on circulating erythrocytes for prophylactic fibrinolysis. Blood 2006;108:1895–902. [PubMed: 16735601]

10. Cesarman-Maus G, Hajjar KA. Molecular mechanisms of fibrinolysis. Br J Haematol 2005;129:307–21. [PubMed: 15842654]

11. Weisel JW, Litvinov RI. The biochemical and physical process of fibrinolysis and effects of clot structure and stability on the lysis rate. Cardiovasc Hematol Agents Med Chem 2008;6:161–80. [PubMed: 18673231]

12. Collet JP, Park D, Lesty C, Soria J, Soria C, Montalescot G, Weisel JW. Influence of fibrin network conformation and fibrin fiber diameter on fibrinolysis speed: dynamic and structural approaches by confocal microscopy. Arterioscler Thromb Vasc Biol 2000;20:1354–61. [PubMed: 10807754]

13. Collet JP, Lesty C, Montalescot G, Weisel JW. Dynamic changes of fibrin architecture during fibrin formation and intrinsic fibrinolysis of fibrin-rich clots. J Biol Chem 2003;278:21331–5. [PubMed: 12642590]

14. Gersh KC, Nagaswami C, Weisel JW. Fibrin network structure and clot mechanical properties are altered by incorporation of erythrocytes. Thromb Haemost 2009;102:1169–75. [PubMed: 19967148]

15. Ding BS, Hong N, Murciano JC, Ganguly K, Gottstein C, Christofidou-Solomidou M, Albelda SM, Fisher AB, Cines DB, Muzykantov VR. Prophylactic thrombolysis by thrombin-activated latent prourokinase targeted to PECAM-1 in the pulmonary vasculature. Blood 2008;111:1999–2006. [PubMed: 18045968]

16. Kina T, Ikuta K, Takayama E, Wada K, Majumdar AS, Weissman IL, Katsura Y. The monoclonal antibody TER-119 recognizes a molecule associated with glycophorin A and specifically marks the late stages of murine erythroid lineage. Br J Haematol 2000;109:280–7. [PubMed: 10848813]

17. Zaitsev S, Spitzer D, Murciano J-C, Ding B-S, Tliba S, Kowalska MA, Bdeir K, Kuo A, Stepanova V, Atkinson JP, Poncz M, Cines DB, Muzykantov VR. Targeting of a mutant plasminogen activator to circulating red blood cells for prophylactic fibrinolysis. J Pharmacol Exp Ther. 2009 DOI:10.1124/jpet.109.159194.

18. Gregory, TR. Cell Size Database. http://www.genomesize.com/cellsize/ 2005

19. Sakharov DV, Nagelkerke JF, Rijken DC. Rearrangements of the fibrin network and spatial distribution of fibrinolytic components during plasma clot lysis. Study with confocal microscopy. J Biol Chem 1996;271:2133–8. [PubMed: 8567670]

20. Ganguly K, Murciano JC, Westrick R, Leferovich J, Cines DB, Muzykantov VR. The glycocalyx protects erythrocyte-bound tissue-type plasminogen activator from enzymatic inhibition. J Pharmacol Exp Ther 2007;321:158–64. [PubMed: 17215448]

21. Weisel JW, Nagaswami C, Makowski L. Twisting of fibrin fibers limits their radial growth. Proc Natl Acad Sci USA 1987;84:8991–5. [PubMed: 3480524]

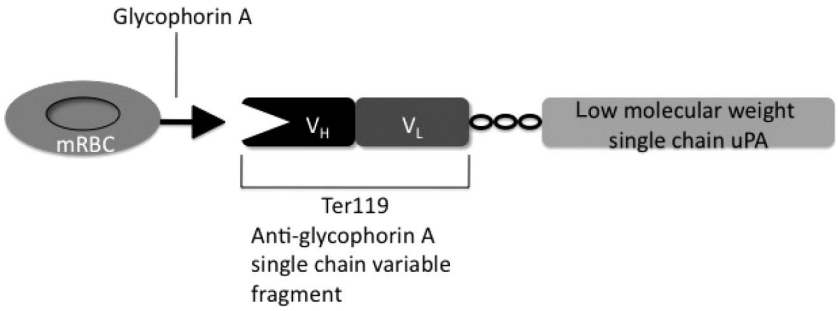

Fig. 1.

Schematic diagram of the plasminogen activator (PA) fusion protein's interaction with glycophorin A on the surface of Mouse red blood cells (mRBCs).

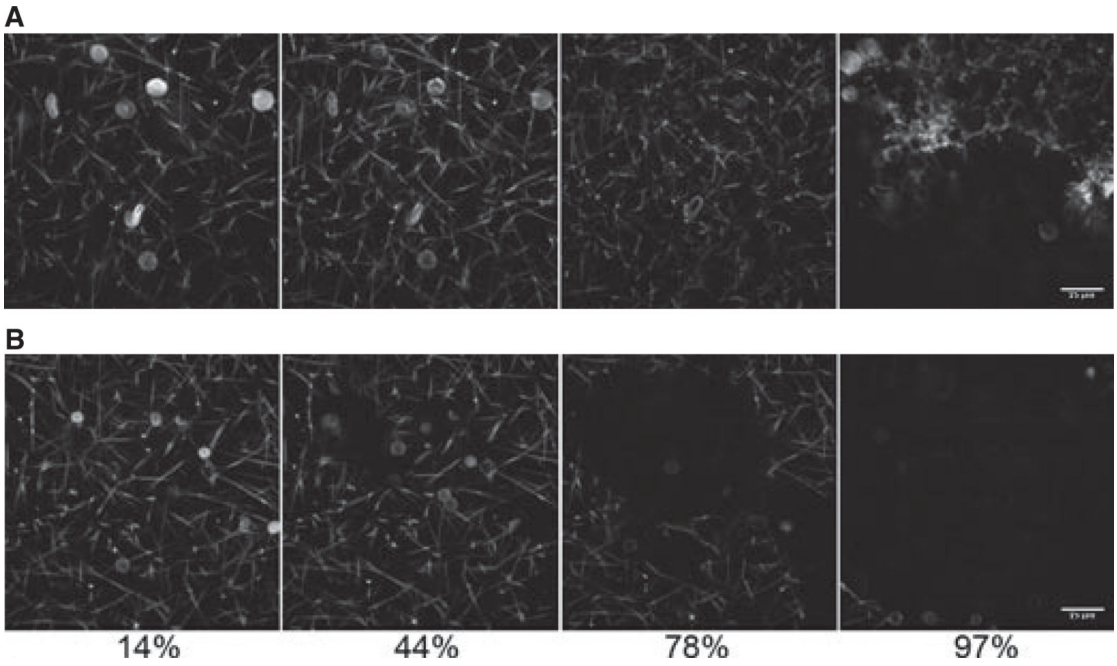

Fig. 2.

Lysis by red blood cell-plasminogen activator (RBC-PA) differs from lysis by free PA. Lysis by free PA (0.00820 μM, final conc) + 1% human RBCs (hRBCs) (A) or 1% RBC-PA (B) as a function of time visualized by spinning disk confocal microscopy. Times are % of the total time required to achieve complete clot dissolution (25 min for free PA and 41 min for RBC-PA). These images are representative of six RBC-PA and nine free PA experiments.

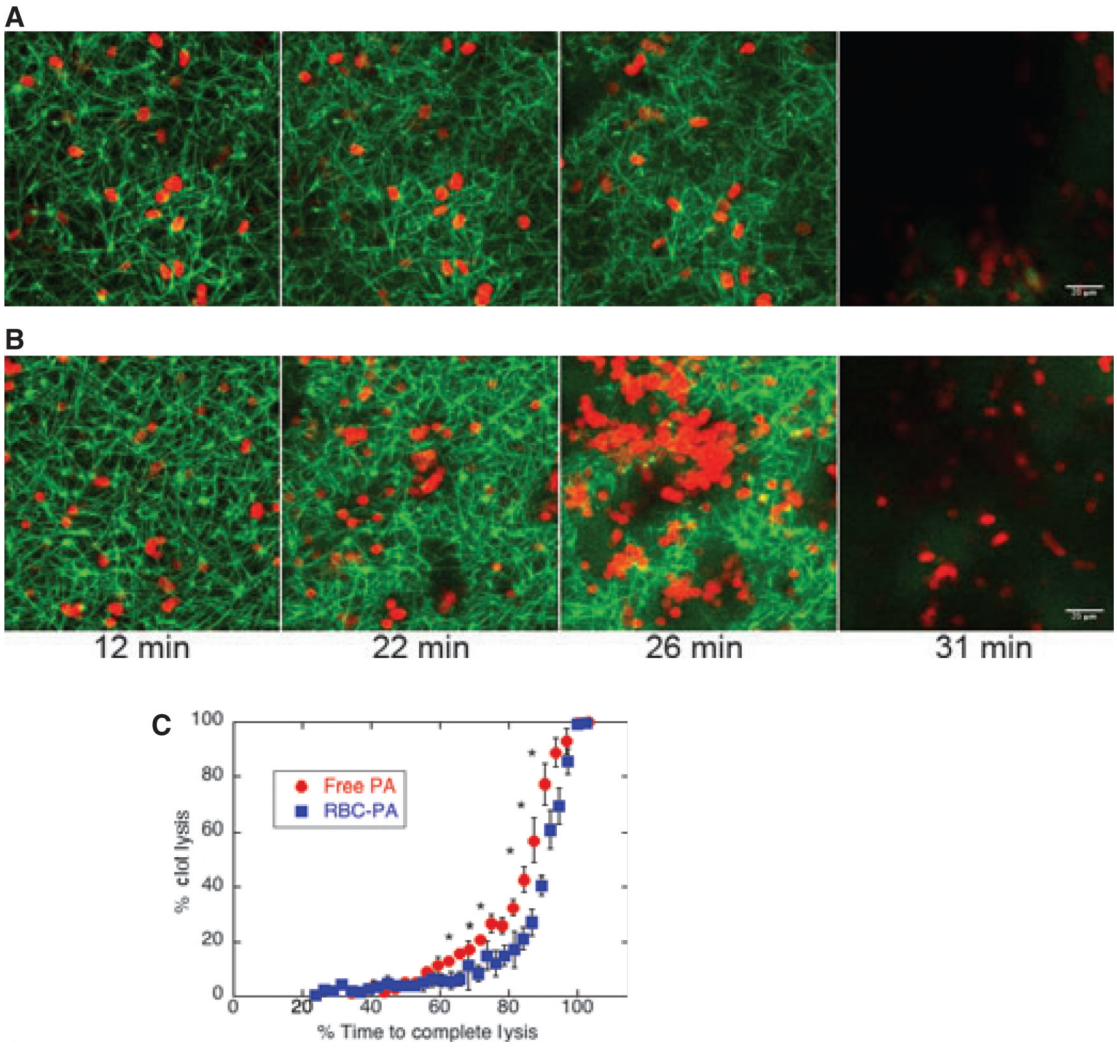

Fig. 3.

Lysis by red blood cell-plasminogen activator (RBC-PA) differs quantitatively from lysis by free PA. Lysis catalyzed by free PA (0.00902 μM, final conc) + 2% hRBCs (A) or 2% RBC-PA (B) visualized by confocal microscopy. In these particular images, representative of 10 free PA and six RBC-PA experiments, both networks achieved dissolution at 31 min. (C) A plot of average % clot lysis vs. a relative scale of % time to complete network dissolution. Error bars are standard error of the mean. **P* < 0.05 for comparison of RBC-PA with free PA (independent *t*-test; *n* = 6 for RBC-PA and *n* =10 for free PA).

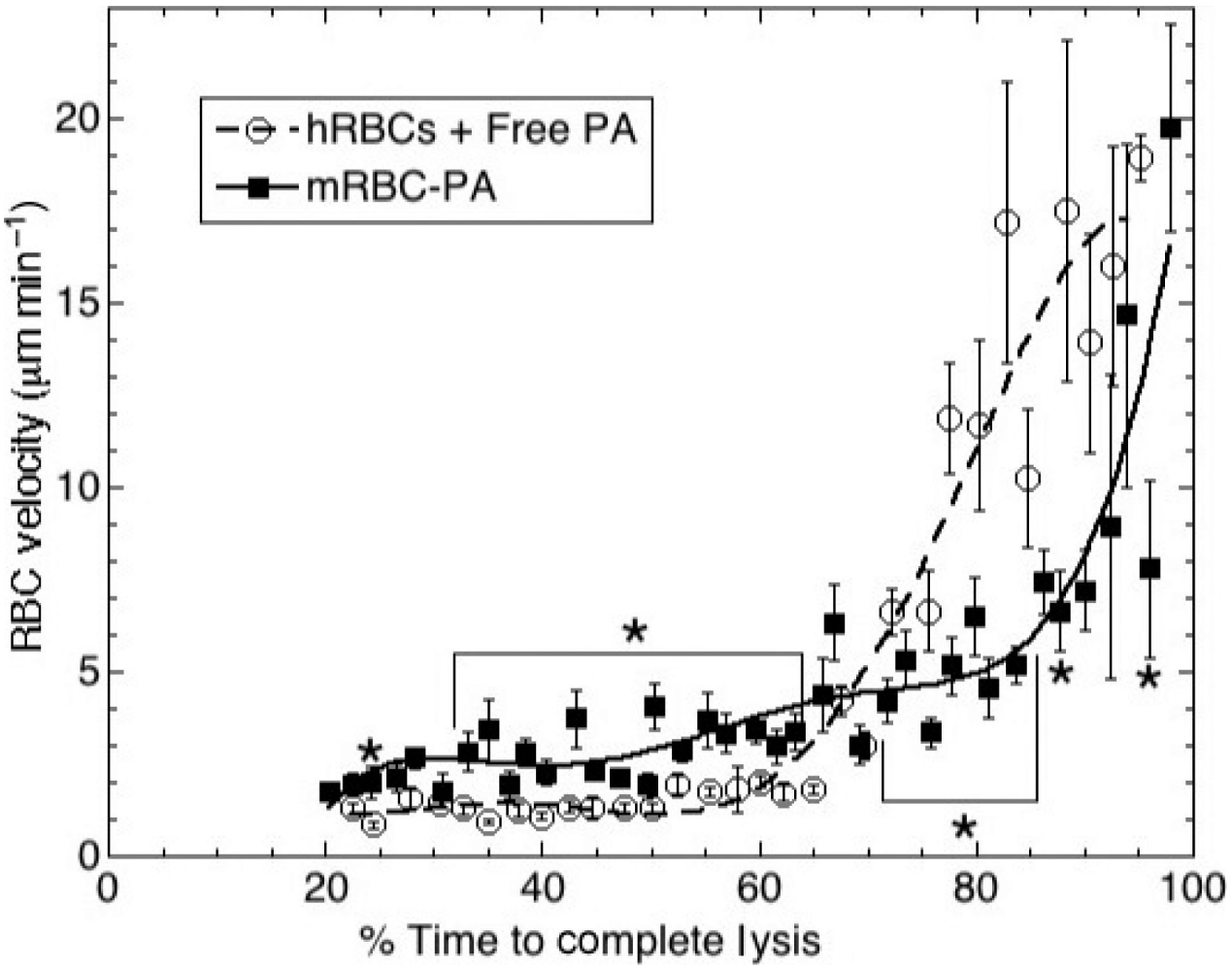

Fig. 4.

Red blood cell-plasminogen activator (RBC-PA) are more mobile within the clot prior to its destruction than are naïve RBCs with free PA. RBC velocity plotted vs. % time requiredtoachieve complete clot dissolution. Error bars are standard error of the mean. *P < 0.05 for comparison of RBC-PA movement with RBCs + free PA movement at the same point in time (independent t-test; n =63 RBCs from seven experiments for RBC-PA; n = 102 RBCs from 10 experiments for free PA). Brackets are used to show intervals in which $P < 0.05$ for comparison of RBC-PA with free PA at every time point within the indicated region.

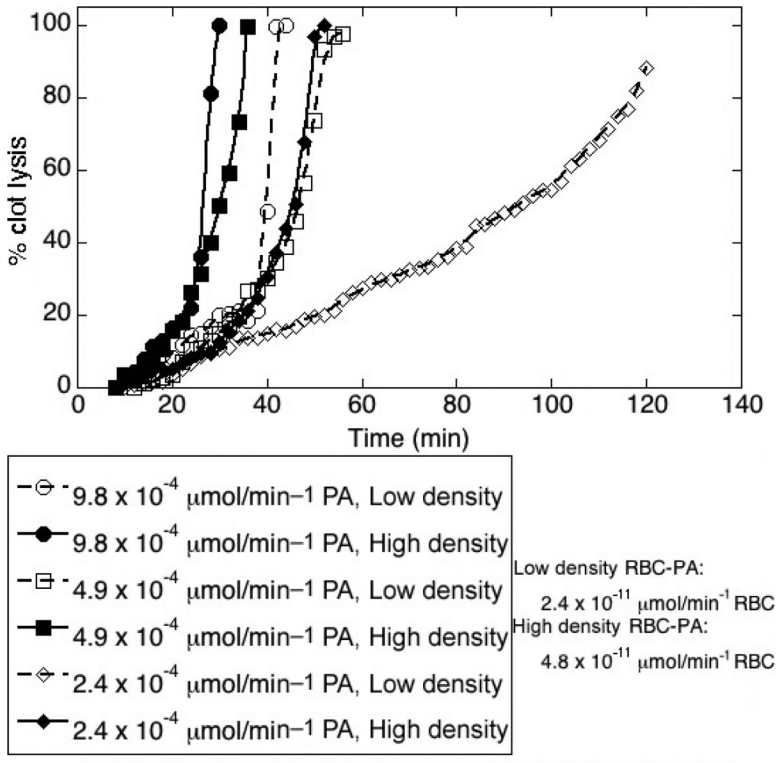

Fig. 5.

Densely-loaded red blood cell-plasminogen activator (RBC-PA) triggers more profound fibrinolysis than a similar dose of sparsely-loaded RBC-PA. Data are shown as % clot lysis vs. time (min). Fibrinolysis was monitored after addition of three different total amounts of PA loaded either sparsely or densely onto RBC-PA. Results are representative of four individual experiments.

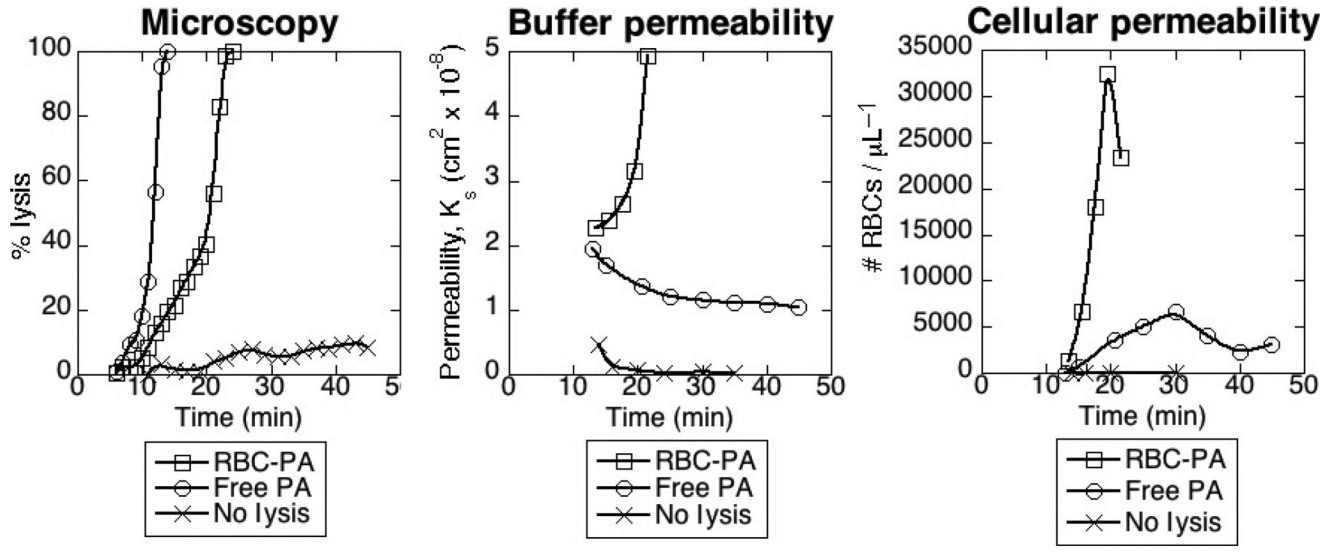

Fig. 6.

Red blood cell-plasminogen activator (RBC-PA), but not free PA, incorporated into clots provides reperfusion in a flow system. (A) Fibrinolysis monitored by quantitative confocal microscopy triggered by free PA (0.0344 μM, final conc) + 2% hRBCs, 2% RBC-PA (equivalent to 0.136 μM uPA), or non-lysing control + 2% hRBCs in a static model system. (B) Permeability constant for liquid perfusion in the flow system for the same samples as (A). (C) Permeability for cellular components, represented as the number per μL of buffer-derived RBCs that permeated the clot during lysis. Plots are representative of six (A, B) and three (C) independent experiments.